Size-based chromatography of signaling clusters in a living cell membrane

Niña G. Caculitan[‡1], Hiroyuki Kai[‡1], Eulanca Y. Liu[‡1], Nicole Fay[1], Yan Yu[1,2,3], Theobald Lohmüller[1,2,4], Geoff P. O'Donoghue[1], Jay T. Groves[1, 2]*

Howard Hughes Medical Institute, Department of Chemistry[1], University of California, Berkeley, California 94720, and the Physical Biosciences and Materials Sciences Divisions[2], Lawrence Berkeley National Laboratory, Berkeley, California USA 94720

[‡] These authors contributed equally to this work.

[3] Present address: Department of Chemistry, Indiana University, Bloomington, IN USA 47405

[4] Present address: Department für Physik und CeNS, Ludwig-Maximilians-Universität, München, München, Germany

[*] Correspondence and requests for materials should be sent to jtgroves@lbl.gov.

KEYWORDS: Membrane, cluster chromatography, T cell receptor, nanodot array

MATERIALS AND METHODS

Fabrication of gold (Au) nanodot array

Au nanodot arrays were deposited on glass substrates according to the method previously reported[1]. In addition, the array with 40 nm spacing was fabricated as follows. Toluene (60.5 mL, Sigma-Aldrich) was added to PS-b-P2VP (M_n(PS) = 7.9 × 10^4, M_n(PVP) = 3.65 × 10^4; 302 mg, 2.6 μmol, Polymer Source) in a capped glass vial and the mixture was stirred overnight at room temperature for complete dissolution. Chloroauric acid hydrate ($HAuCl_4$) (Sigma-Aldrich, 154.2 mg, 0.45 mmol; $[HAuCl_4]/[VP]_{PVP}$ = 0.50) was added to the polymer solution and stirred overnight at 40°C. Glass coverslips (diameter = 40 mm, Bioptechs) were sonicated in IPA/water for 30 min, rinsed with water, and immersed in piranha solution (H_2O_2:H_2SO_4 = 1:3) for 15 min. Coverslips were then rinsed copiously with water and dried with a stream of nitrogen gas. Within 45 min, one-half of the substrate was dip-coated in the Au micelle solution. The substrate was then plasma irradiated using a plasma cleaner (PDC-32G, Harrick Plasma) operated at 18 W for 90 min to remove the polymer and reduce the Au salt to form the nanodot array. Sample substrates from each batch were imaged by scanning electron microscopy (SEM) on a Hitachi S-5000 operated at 10 kV acceleration voltage. Interparticle spacing was calculated using particle detection by threshold on ImageJ followed by nearest neighbor detection by Delaunay triangulation algorithm[2] (Fig. S1; Source code is available at https://github.com/hirokai/Delaunay). Polymers and dip-coating speeds were varied accordingly for different spacings (Table S2).

Preparation of T cells

AND $CD4^+$ T cells were harvested from lymphocytes and splenocytes of F1 generation AND × B10.Br mice (Jackson Laboratory) 6-13 weeks of age and expanded to T cell blasts as previously described[3]. This protocol is approved by the Animal Welfare and Research Committee (AWRC) under Animal Use Protocol #177002.

Preparation of proteins

Histidine-tagged intercellular adhesion molecule-1 (ICAM-1) and major histocompatibility complex (MHC) Class II I-E^k proteins were expressed and purified as before[4]. Fab fragments derived from H57 anti-T cell receptor (TCR) antibodies were prepared by standard protocols. Moth cytochrome c (MCC) agonist peptide (ANERADLIAYLKQATK) and/or T102E (ANERADLIAYLKQAEK) null peptide were loaded onto MHC at 100 μM in pH 4.5 citrate buffer and incubated at 37°C 48 hours prior to pMHC incubation with the supported lipid bilayer (supported membrane). For pMHC imaging experiments, MCC-C (ANERADLIAYLKQATKGGSC) was used instead of MCC. Conjugation of ICAM-1 with Alexa Fluor 488 (AF488), anti-TCR Fab with Alexa Fluor 594 (AF594), and MCC-C with Alexa Fluor 488 maleimide was performed according to Molecular Probes instructions.

Preparation of supported lipid bilayers

Substrates with the Au nanodot array prepared above were irradiated with air plasma for 5 min to activate the surface and were used as the bottom face of an enclosed, temperature-controlled flow cell system (FCS2, Bioptechs). The entire surface was covered with a

supported membrane spontaneously formed with the addition of small unilamellar vesicles of 1,2-dioleoylphosphotidylcholine (DOPC) containing 2 mol% 1,2-dioleoyl-*sn*-glycero-3-[(N-(5-amino-1-carboxypentyl) iminodiacetic acid) succinyl] (nickel salt) (Ni-DOGS) (Avanti Polar Lipids) prepared by standard methods[5]. ICAM-1 and pMHC were loaded on the supported membrane with a 40 min incubation at room temperature followed by a 1x tris buffered saline solution rinse to wash away unbound proteins. For ag:null titration experiments, ag pMHC and null pMHC solutions were added according to the ratios indicated.

TCR tracking experiment

Primary murine T cells were incubated with AF594 anti-TCR Fab fragments for 20 min on ice, then injected into the flow cell at 37°C containing the supported membrane prepared above. Total internal reflection fluorescence (TIRF) microscopy images were taken using Orca-R2 CCD camera (C10600-10B, Hamamatsu Photonics K.K.) with a 561 nm laser source (GCL-100-561, CrystaLaser) at a rate of 1 s^{-1} with 500 ms exposure time. Particle tracking of the images was performed using a MATLAB script[6] and u-track software[7].

Fixed cell experiment

T cells were stained and incubated with the supported membrane as above at 37 °C for 20 min, then fixed with 2% paraformaldehyde for 10 min. Cells were then imaged using a 100x oil immersion objective and corresponding filter cubes. Epifluorescence images were captured using CoolSNAP HQ CCD camera (Photometrics) using MetaMorph software package (Molecular Devices). TIRF images were captured using Orca-R2 CCD camera with 488 nm argon-ion laser (177g, Spectra Physics) and 561 nm optically-pumped solid state laser (Coherent Sapphire) as the laser sources.

Image analysis

The radial profile of the TCR image of every cell was calculated by a program that was developed on the ImageJ platform. (http://github.com/hirokai/TCRAnalysis). Variance of the radial profile of every cell, σ^2, is defined for the symmetrized radial profile, $P(r)$, by the equation,

$$\sigma^2 \equiv \int_{-1}^{1} r^2 P(r) dr, \qquad \text{where } P(r) \equiv \frac{p(|r|)}{2}. \left(\int_{-1}^{1} P(r) dr = 1, \int_{-1}^{1} r P(r) dr = 0 \right)$$

Radial profiles were averaged over all the cells (n ≥ 39, typically n > 100) on and off the nanodot array respectively. Variance of the radial profile was collected to plot a histogram, and analyzed by R software for statistical significance.

Calcium signaling experiment

Non-fluorescent ICAM-1 was loaded onto the supported membrane along with pMHC as described above. Cells were first incubated with 1 μM fura-2-acetoxymethyl ester (Fura-2 AM, Molecular Probes) in FBS-free media for 15 min at room temperature and incubated with serum rich media at 37°C for 20 min. Cells were then labeled with AF594 anti-TCR antibody as above. Intracellular calcium flux was monitored with excitation wavelengths of 340 and 380 nm and emission of 510 nm using a 40x objective with

CoolSnap K4 camera as before[8]. Time course of Fura-2 340/380 fluorescence intensity ratio of every cell was analyzed by Imaris software and the intensity profiles were plotted as heatmaps by a MATLAB script.

Supplementary Discussion 1

We know from prior studies that interference with TCR cluster movement can induce minor perturbations on cell signaling[1,2,3]. However, our experiments aim to map the boundary of conditions at which frustration first occurs in order to map the size of the TCR cluster. Thus, from the point of view of the experiment, there is no need to interpret what happens in the T cell after the TCR cluster transport has been impeded.

Supplementary Discussion 2

In an early study of TCR microclusters[4], it was reported that TCR cluster size exhibits minimal differences over a hundred-fold variation of average pMHC density from 0.2–20 molecules/μm^2. However, it was later realized that the GPI-linked pMHC proteins used in this study (and others) have a tendency to aggregate in supported membranes[5,6]. Thus titrating the average density of gpi-linked pMHC does not reduce the number of pMHC per TCR cluster at low densities. The polyhistidine linkage to Ni-NTA lipids does not lead to any preclustering, as is clearly indicated by direct single molecule imaging of peptide-labeled pMHC complexes in supported membranes (S10).

Reference	Activating Surface	# ag pMHC	Method	Microcluster analysis	TCR labeling	Size of TCR domains	#TCRs/domain	# cells tested
Yokosuka et al, *Nat. Imm.* 2005	Bilayer with GPI-anchored ICAM-1 and pMHC	density was "2.3-fold higher than that on activated B cells"; varied peptide in solution (0.8 μM, 4 μM, 20 μM, 100 μM)	Total internal reflection fluorescence microscopy	Fluorescence intensity based analysis relative to single eGFP molecule	CD3ζ-EGFP	not mentioned	After >10 min: 40-110 at periphery, 110-290 near cSMAC	~10
Campi et al., *JEM*, 2005	Bilayer with GPI-anchored ICAM-1 and pMHC	40 pMHC/μm^2	Total internal reflection fluorescence microscopy	H57 binding sites by FACS show ~140 TCR/μm^2 on cell; Microclusters 2x the avg. intensity of pMHC at 50 mol/μm^2; therefore 140 TCR/microluster initially	H57 anti-TCR f_{ab} fragment	0.35-0.5 um^2	After a few min: 140	>20
Varma et al., *Immunity* 2006	Bilayer with GPI-anchored ICAM-1 and pMHC	varied from 0.2 pMHC/μm^2 to 20 pMHC/μm^2	Total internal reflection fluorescence microscopy	Fluorescence intensity method as before, but after 30 min	H57 anti-TCR f_{ab} fragment	not mentioned	After 30 min: 11 TCR for 0.2 pMHC/μm^2; 17 TCR for 20 pMHC/μm^2	25
Lillemeier et al., *Nat. Imm.* 2010	Immobilized ICAM-1, B7-1, and pMHC on poly-L-lysine	18,500-21,500 pMHC/μm^2	high speed photoactivated localization microscopy	probability density peaks	CD3ζ-PSCFP2	35-70 nm radius	70to 300	15-20
Lillemeier et al., *Nat. Imm.* 2010	Bilayer with histidine-tagged ICAM-1, B7-1, and pMHC	30 pMHC/μm^2	high speed photoactivated localization microscopy	probability density peaks	CD3ζ-PSCFP2	35-70 nm radius	70 to 200	15
Lillemeier et al., *Nat. Imm.* 2010	Immobilized B7-1, and pMHC on poly-L-lysine	18,500-21,500 pMHC/μm^2	Transmission electron microscopy	Ripley's *K*-function analysis	Anti-CD3ζ-Au particle	40-300 nm radius	7 to 30	25-30

Table S1. Summary of past studies that investigate TCR domain size.

Average spacing obtained	Molecular weight of polymer		Concentration of polymer [mg/mL]	Loading ratio	Dip-coating speed [mm/min]
	M_n (PS)	M_n (PVP)			
40-50 nm	7.9×10^4	3.7×10^4	5	0.5	42
81 nm	1.1×10^5	5.2×10^4	6		36
120 nm	1.1×10^5	5.2×10^4	4		24
143 nm	1.1×10^5	5.2×10^4	4		12
171 nm	1.1×10^5	5.2×10^4	2		24

Table S2. Conditions used for the fabrication of gold nanoparticle arrays to achieve various interparticle spacings. Polymers used: Polymer Source P4633-S2VP (for 40-50 nm spacings) and P5922-S2VP (for >80 nm spacings). A few samples from each batch of fabricated substrates were imaged by scanning electron microscopy (SEM) and analysed to determine the average nanodot spacing. Values for the average spacing can fluctuate from different batches of fabrication using the same condition.

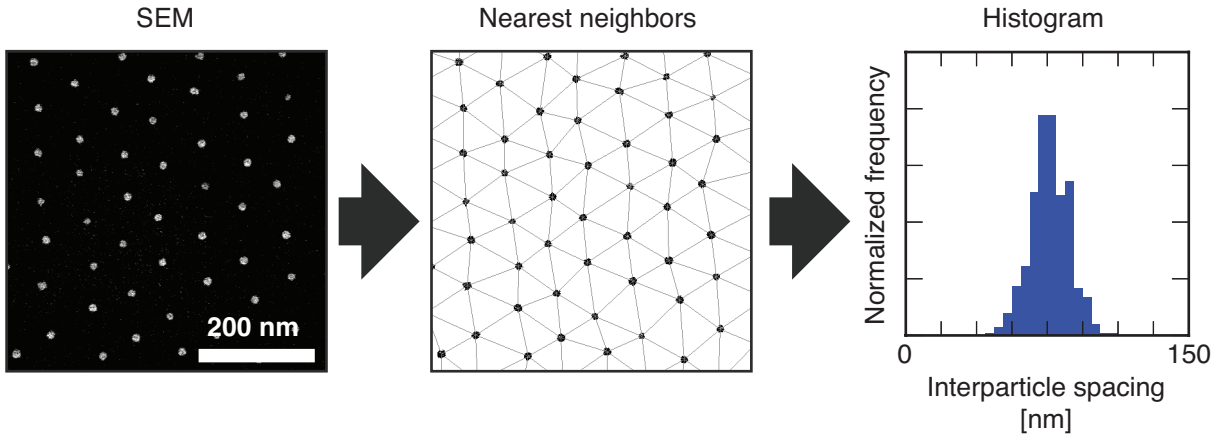

Figure S1. **Schematic for the analysis of gold nanodot spacing from SEM images.** Scanning electron microscopy (SEM) images were analyzed using nearest neighbors detection by Delaunay triangulation algorithm. The distribution of distances was collected to produce a histogram.

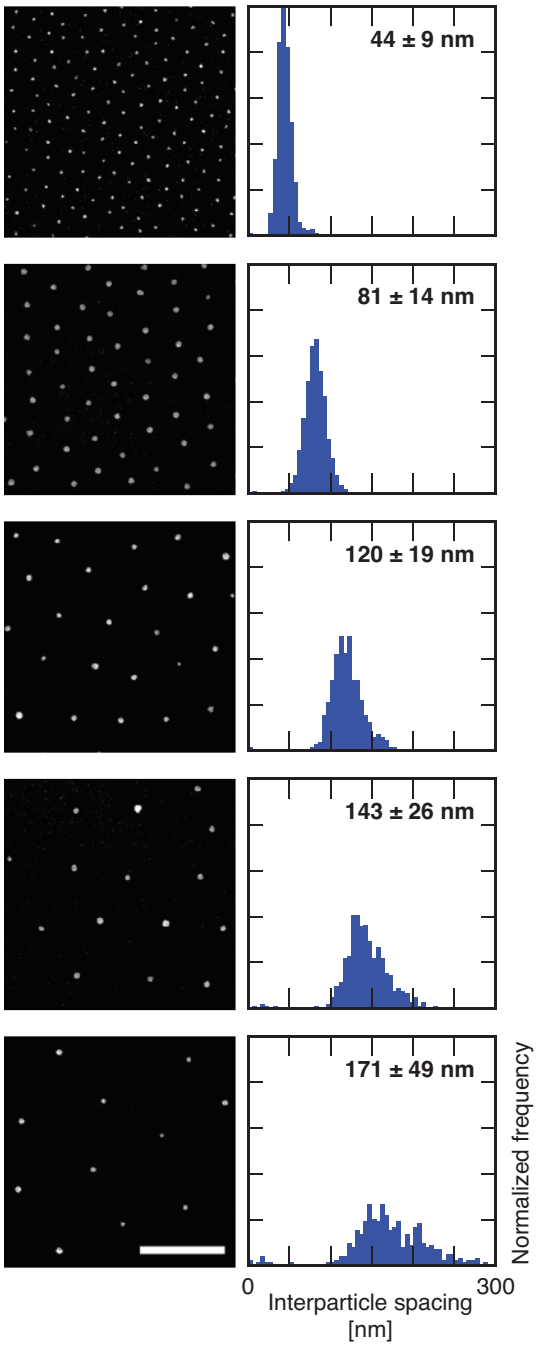

Figure S2. Histogram analyses for nanodot arrays at various spacings. SEM images of nanodot arrays (left), and histograms for the distribution of distances (right). Calculated mean and standard deviation of interparticle spacings are shown. Scale bar: 200 nm.

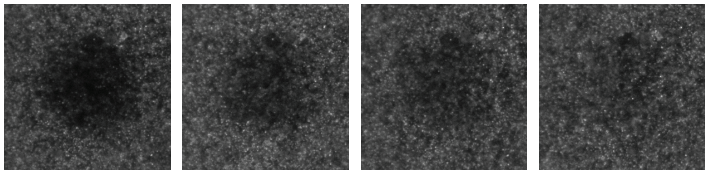

Figure S3. The supported membrane is fluid on the nanodot array. Fluorescence recovery after photobleaching (FRAP) images of Alexa fluor labeled MCC peptide bound to major histocompatibility complex (MHC) proteins presented on the supported membrane with the nanodot array prior to T cell addition. Supported membranes consist of a continuous phospholipid bilayer that coats the surface of a solid substrate, such as silica or some polymers. A thin water layer separates the membrane from the underlying substrate, allowing free lateral mobility of lipids and membrane-linked proteins.

a

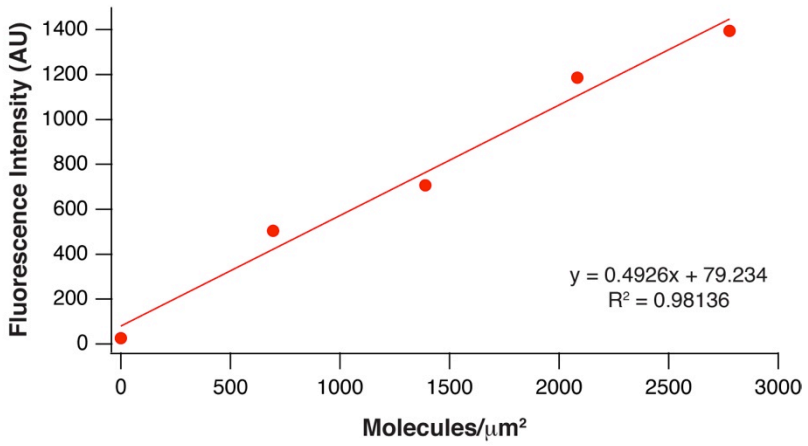

b

Average Intensity MCC-C-AF568 (AU)	125.27
Texas Red/Alexa Fluor 568 correction factor	1.1195
Calculated bilayer [MCC-C] (molecules/μm^2)	83.54

Figure S4. Calculation of the density of MCC-loaded MHC molecules on the supported membrane. Quantitative fluorescence analysis was used to determine the surface of MCC-loaded MHC molecules. **a** The surface density calibration standard was generated using supported membranes doped with Texas Red at various concentrations. b The concentration of Alexa Fluor 568 labeled MCC-loaded MHC on the bilayer (83 molecules/μm^2) was calculated using the equation derived from a and values shown in **b**.

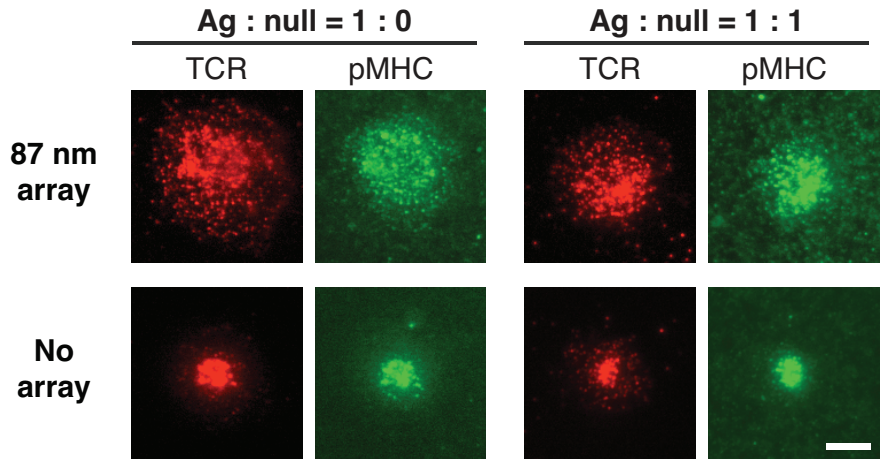

Figure S5. TCR and pMHC on and off the nanodot array. Total internal reflection fluorescence (TIRF) microscopy images of the T cell receptor (TCR) on the cell membrane and MCC-MHC on the supported membrane on and off the nanodot array at different agonist:null peptide ratios. Scale bar: 5 μm.

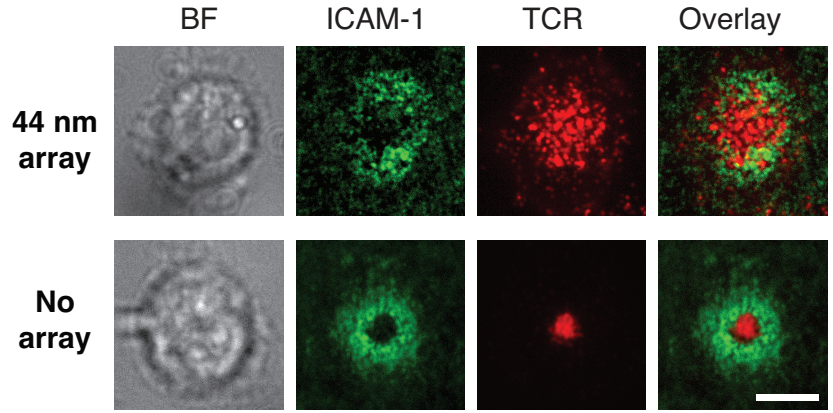

Figure S6. ICAM-1 still forms a ring on the nanodot array. Bright field and epifluorescence images of TCR and intercellular adhesion molecule-1 (ICAM-1) on a supported membrane embedded with or without a nanodot array. Scale bar: 5 μm.

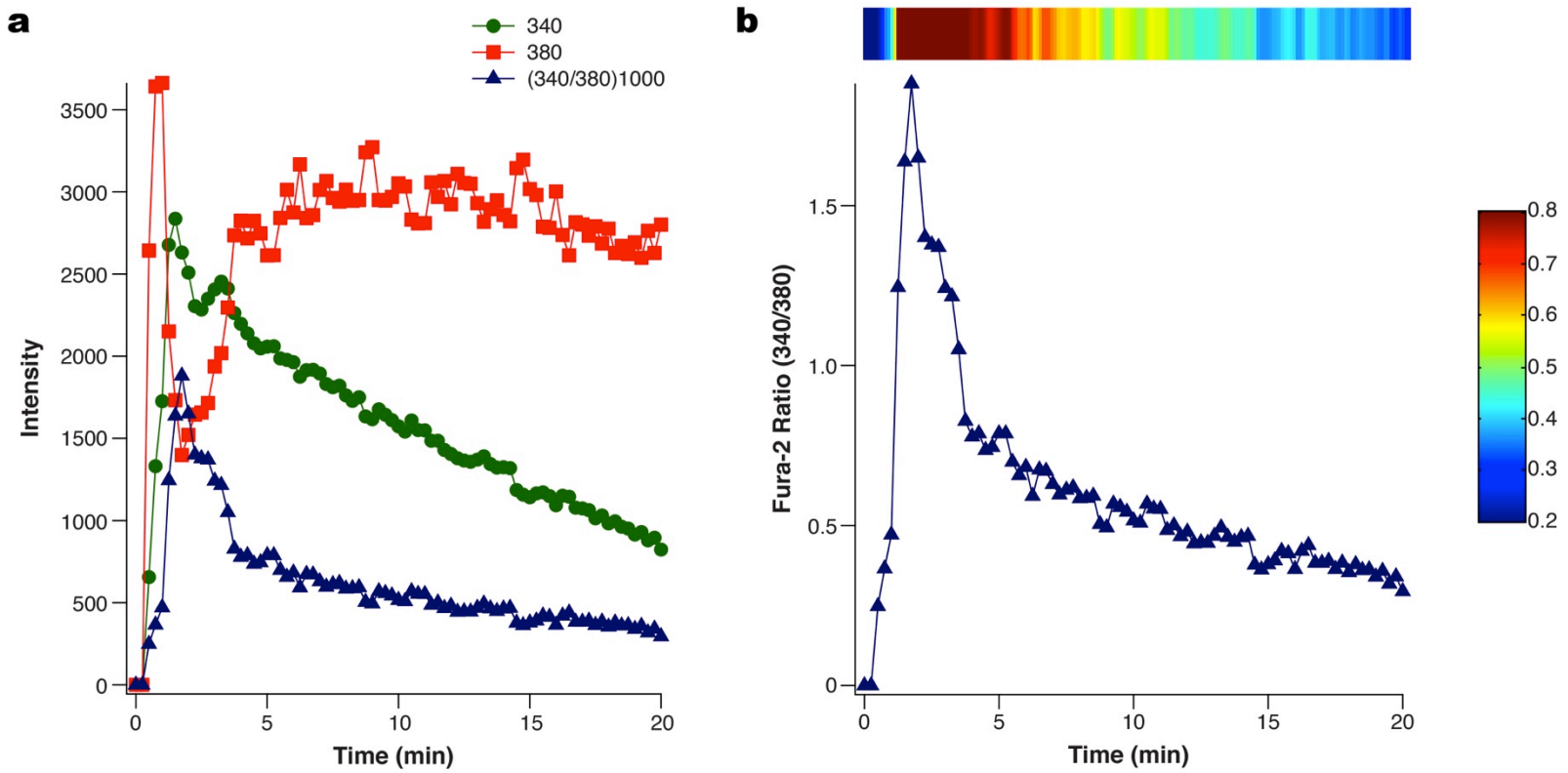

Figure S7. Quantification of calcium flux. **a** Calcium flux for a single cell on a bilayer. Curves for Fura-2 AM excitation at 340 nm (green) and 380 nm (red), both with emissions collected at 510 nm. The calculated curve for the Fura-2 ratio (340/380) is shown (blue). **b** Curve of the Fura-2 ratio (blue) and corresponding heat map trace for a single cell. A heat map for all the Fura-2 ratio traces is generated to display all the Ca^{2+} flux data for a large number of cells per condition.

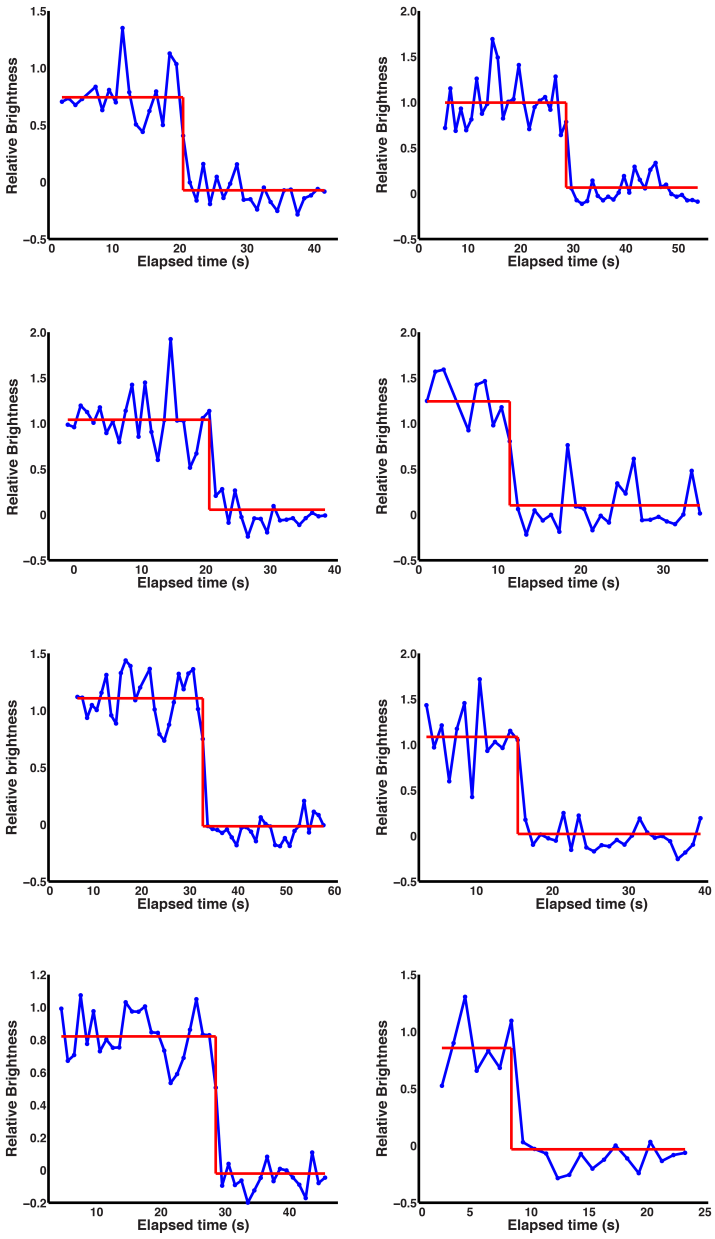

Figure S8. MHC linked via Ni-NTA lipids to the supported membrane are not preclustered. Collection of single molecule traces for individual pMHC molecules. The red line denotes intensity levels detected using a Bayesian change point technique* and a Bayes Factor of 25. Data were collected at 17.5 ms intervals. Discrete single-step photobleaching observed for all molecules indicate that the pMHC exists ~100% as a monomer.

*Ensign, D. L. & Pande, V. S. Bayesian Detection of Intensity Changes in Single Molecule and Molecular Dynamics Trajectories. The Journal of Physical Chemistry B 114, 280–292 (2010).

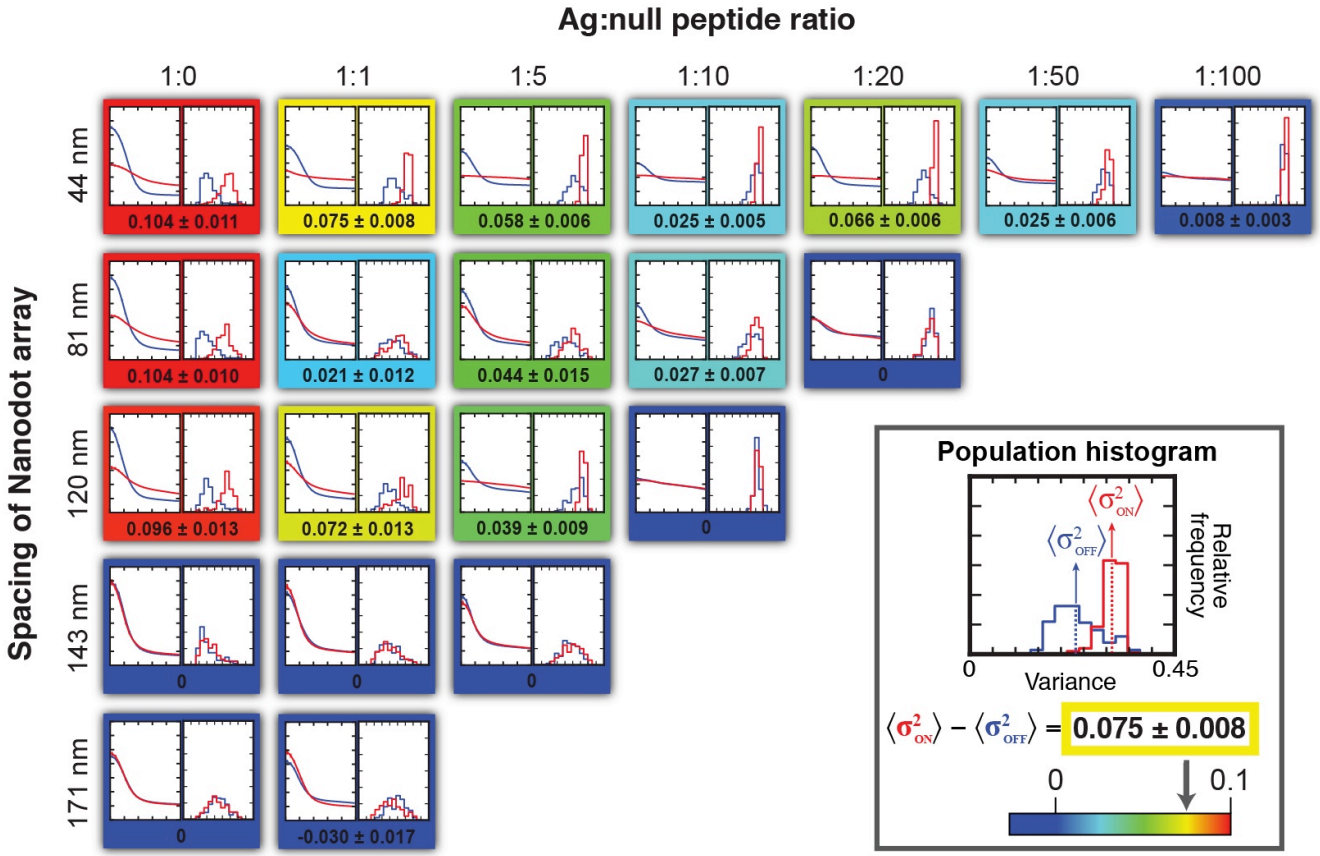

Figure S9. Cell population analyses of TCR microcluster transport as a function of nanodot array spacing and agonist peptide density on the supported membrane. The graph on the left is the average radial profile on (red) and off (blue) the array. The graph on the right is the population histogram generated per condition. The colored borders indicate the difference in variance off and on the nanodot array.

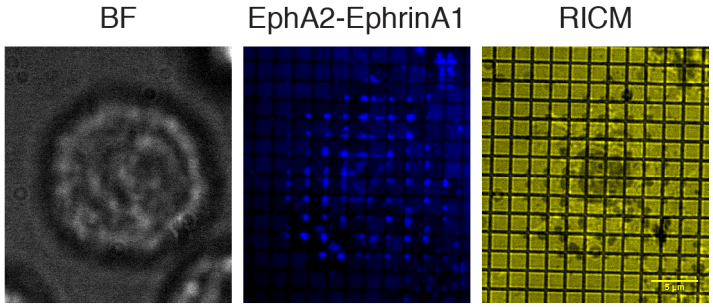

Figure S10. EphA2-ephrinA1 clusters induce large topographical differences at the membrane-membrane interface. TIRF image of Alexa Fluor 647 labeled-ephrinA1 bound to its EphA2 receptor. Cluster transport is restricted by chromium lines that allow lipid and protein mobility only within the corrals. The RICM image reveal punctate topographical features that correspond with the EphA2-ephrinA1 clusters.

References

(1) Lohmüller, T. et al. Supported Membranes Embedded with Fixed Arrays of Gold Nanoparticles. *Nano Lett*. **11,** 4912–4918 (2011).

(2) Chew, L.P. Voronoi Diagram / Delaunay Triangulation. http://www.cs.cornell.edu/info/people/chew/Delaunay.html (accessed Mar 11, 2014)

(3) Mossman, K. D., Campi, G., Groves, J. T. & Dustin, M. L. Altered TCR signaling from geometrically repatterned immunological synapses. *Science* **310,** 1191–1193 (2005).

(4) Hartman, N. C., Nye, J. A. & Groves, J. T. Cluster size regulates protein sorting in the immunological synapse. *Proc. Natl. Acad. Sci. USA* **106,** 12729–12734 (2009).

(5) Lin, W.-C., Yu, C.-H., Triffo, S. & Groves, J. T. Supported Membrane Formation, Characterization, Functionalization, and Patterning for Application in Biological Science and Technology. *Curr. Protoc. Chem. Biol*. (2010).

(6) Yu, Y., Fay, N. C., Smoligovets, A. A., Wu, H.-J. & Groves, J. T. Myosin IIA Modulates T Cell Receptor Transport and CasL Phosphorylation during Early Immunological Synapse Formation. *PLoS ONE* **7,** e30704 (2012).

(7) Jaqaman, K., Loerke, D.,Mettlen, D., Kuwata, H., Grinstein, S., Schmid, S. L. & Danuser, G. Robust single-particle tracking in live-cell time-lapse sequences. *Nat. Methods* **5,** 695–702 (2008).

(8) Nye, J. A. & Groves, J. T. Kinetic control of histidine-tagged protein surface density on supported lipid bilayers. *Langmuir* **24,** 4145–4149 (2008).